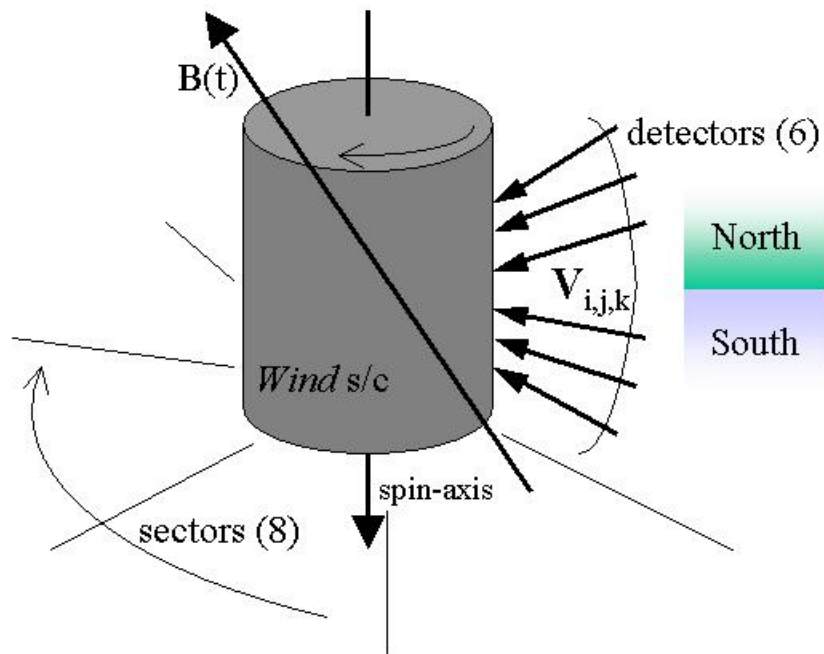


Wind/SWE “New mode” Electron Pitch-angle Analysis

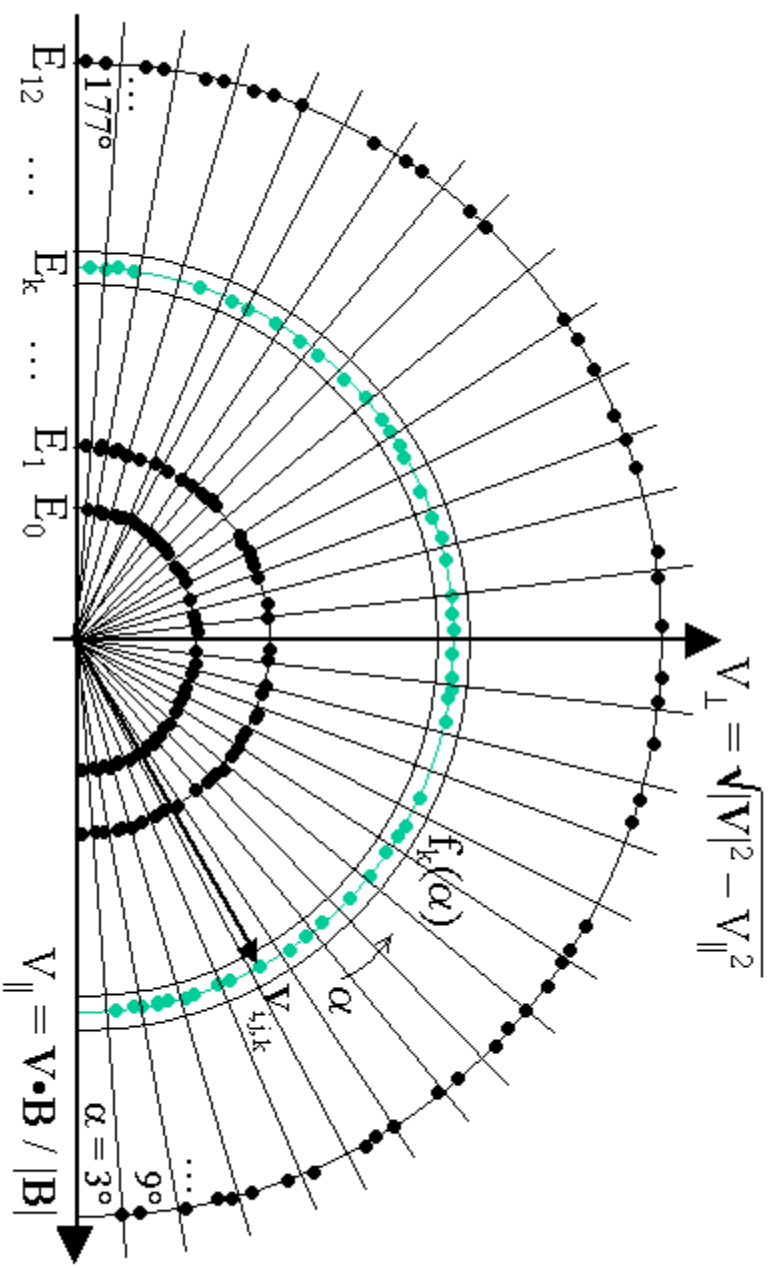
Overview

Effectively, in this mode of the electron instrument, there are 13 energy-channels (electron speeds) making 48 observations (instrument counts for each particular velocity) over 8 sectors ($\sim 45^\circ$ wide) and 6 elevations ($\sim 9^\circ$ apart) at each energy. From these 624 observations (accumulated over 3 s/c spins, or ~ 9 s) 13 pitch-angle distributions and one “spin-averaged” energy distribution are populated during every ~ 12 s interval.



In the following discussion:

- The observed energies are represented as E_0, E_1, \dots, E_{12} . Where E_0, E_1, \dots, E_{10} are observed *once* in each sector; E_{11}, E_{12} are observed *twice*, then averaged. This achieves more statistically meaningful observations in energy-ranges where fewer counts are observed, and accounts for the mapping from the 15 energy-channels in the current operational mode to the 13 channels discussed here.
- $i = 0, 1, \dots, 5$ indexes *detector*.
- $j = 0, 1, \dots, 7$ indexes *sector*.
- $k = 0, 1, \dots, 12$ indexes *energy*.
- \mathbf{B}, \mathbf{V} vectors are given in GSE coordinates, with \mathbf{B} being the temporally “nearest” 3s MFI observation to any given SWE observations of electron \mathbf{V} .
- $\alpha_{i,j,k} = \cos^{-1} \{ \mathbf{V}_{i,j,k} \cdot \mathbf{B}(t) / [|\mathbf{V}_{i,j,k}| |\mathbf{B}(t)|] \}$ gives the pitch-angle for each observation, with $c_{i,j,k}$ giving the corresponding count-value.



During each energy “spectrum”, a velocity distribution (with 13 energy “shells”) is formed. The points shown here suggest the binning process for each shell.

For $E = E_k$, the 30 pitch-angle bins (6° wide) of the k^{th} (of 13) pitch-angle distribution ($f_k(\alpha)$) are populated as follows...

Typically a conversion from counts to phase-space densities requires both energy and a “geometric factor” for each contributing detector. However, acknowledging that the following process unavoidably intermingles counts from different detectors, and that the geometric information from our instrument specifications gives a single conversion factor (call it cf_k) for each energy (E_k), averaged count-values are simply scaled by this factor to yield corresponding phase-space densities:

$$f_k(\alpha) = [\sum c_{i,j,k} / n] cf_k, \alpha = 3^\circ, 9^\circ, \dots, 177^\circ.$$

The summation is carried out over i,j s.t. $\alpha_{i,j,k}$ lies within 3° of the specified center-angle α (e.g. from 0° to 6° for $\alpha = 3^\circ$, 6° - 12° for $\alpha = 9^\circ$, ..., 174° - 180° for $\alpha = 177^\circ$), and n is the number of detectors (observations) contributing counts to the sum.

One additional value is generated for each energy:

$$\langle f \rangle_k = [\sum c_{i,j,k} / N] cf_k$$

where the summation is carried out over *all* i,j and N is the number of detectors contributing counts to this “grand total” sum.

This completes the information needed to generate our electron pitch-angle data product for this mode (very similar to that of previous modes):

$f_0(\alpha), f_1(\alpha), \dots, f_{12}(\alpha)$ for $\alpha = 3^\circ, 9^\circ, \dots, 177^\circ$ (30 6° bins) form the pitch-angle distributions, and $[\langle f \rangle_0, \langle f \rangle_1, \dots, \langle f \rangle_{12}]$ forms the “spin-averaged” energy (speed) distribution, accumulated over each ~ 9 s interval (available about every 12s).

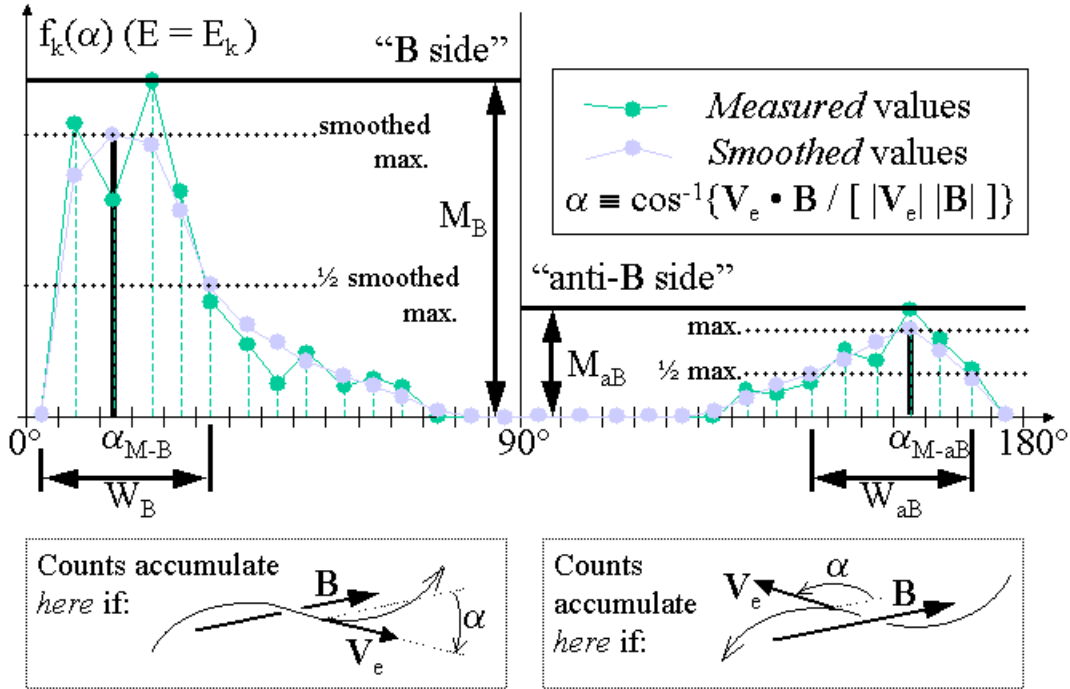
For reference:

- The 6 GSE *particle-velocity direction* elevation angles used in our analysis are: $-26.55^\circ, -17.10^\circ, -7.34^\circ, 7.63^\circ, 17.10^\circ$, and 26.53° (above the ecliptic).
- The 13 electron energies (E_k $k = 0, 1, \dots, 12$) are: 19.34, 38.68, 58.03, 77.37, 96.71, 116.1, 193.4, 290.1, 425.5, 580.3, 773.7, 1006., and 1238. eV.
- The 13 corresponding electron speeds are: 2.61, 3.69, 4.52, 5.22, 5.83, 6.39, 8.25, 10.1, 12.2, 14.3, 16.5, 18.8, and 20.9×10^8 cm/s.

Derived Products

From the electron pitch-angle distribution product described above, there are derived two additional data products: *the ‘strahl’ product* (useful both as a reduced summary of the pitch-angle product, and as an indication of whether the strahl phenomenon is being observed), and *the ‘pitch-average’ product* (another approach to reducing the pitch-angle product, this time by averaging over regimes of interest). Basic derivation and contents of these products is discussed below. Note that, as with the pitch-angle product, these products are very similar to those of previous modes.

Strahl Product: First, recall the 30 pitch-angle bins (6° wide) of the k^{th} (of 13) pitch-angle distribution ($f_k(\alpha)$ for $E = E_k$) populated above...



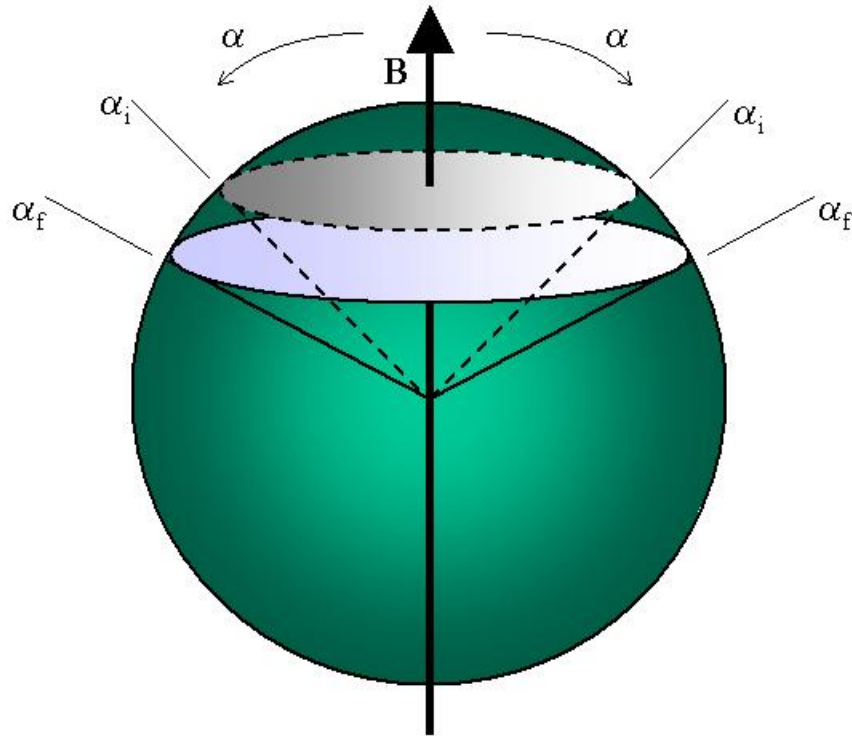
Next, a smoothing operation is applied to the “measured” values. Then we perform the following analysis on both the “**B** side” (the 15 bins associated with forward-streaming electrons) and the “**anti-B** side” (the other 15 bins associated with backward-streaming electrons). The maximum *measured* value is noted (call it M_B , and M_{aB} , respectively); giving a characteristic intensity for each side. After this, the maximum *smoothed* value is noted, as well as the corresponding half-maximum, and a search is conducted starting from this position. We seek the first bin, in each direction, whose value falls at or below the half-maximum value. We call the pitch-positions of the smoothed maxima α_{M-B} , and α_{M-aB} , respectively. The separation of the *half*-maximum bins we call W_B , and W_{aB} , respectively; as they give characteristic widths.

When the strahl phenomenon is being observed, these parameters describe the strahl “beams” being observed. In this case, M^* ($*$ = B or aB) provides a measure (in units of phase-space density) of beam intensity, $\alpha_{M,*}$ provides a representative pitch-angle for each beam, and W^* provides a measure of (angular) beam-width. One typical use of this product (which is entirely consistent with previous modes of the electron instrument) is as an indicator of whether the strahl phenomenon is, in fact, being observed. When the phenomenon *is* being observed, we expect to see relatively intense beams with relatively small deviations from the 0° and 180° pitch-angle positions and relatively small widths. An investigator interested in this phenomenon could focus attention (on the underlying high-resolution data) only where these criteria were met. On

the other hand, this product is always useful as a reduced, summary representation of the pitch-distribution product; as it tends to capture (in a small amount of data) the sort of salient features apparent in our visualizations of the unreduced pitch product.

13 values (from pitch-angle distributions at each energy) of M_B , M_{aB} , α_{M-B} , α_{M-aB} , W_B and, W_{aB} (available about every 12s) form this data product.

Pitch-average Product: Derived, again, from the 30 pitch-angle bins (6° wide) of the k^{th} (of 13) pitch-angle distribution ($f_k(\alpha)$ for $E = E_k$) populated above...



The figure for this section suggests the final approach for reducing our pitch-angle data: *averaging over regimes of interest on the **unit sphere***. This approach begins by identifying 28 annular “strips” (and two “polar caps”) of solid angle by the relation $\alpha_i < \alpha < \alpha_f$, where the α_i and α_f values are the familiar pitch-angle bin boundaries from above. Next, we establish “weights” for our averaging process by calculating:

$$\Omega_m = \int_{\alpha_{i,m}}^{\alpha_{f,m}} [2\pi \sin \alpha] d\alpha = 2\pi [\cos \alpha_{i,m} - \cos \alpha_{f,m}]$$

for the m^{th} pitch-angle bin. Upon finally noting that the $0^\circ < \alpha < 90^\circ$, $60^\circ < \alpha < 120^\circ$, and $90^\circ < \alpha < 180^\circ$ regions all have solid angle 2π str—the entire sphere having solid angle 4π str; we may proceed with averaging. The results (k^{th} pitch-distribution) are:

$$f_{\text{para},k} = 1/2\pi \sum_{m=0,14} [f_k(\alpha_m) \Omega_m], \text{ (“parallel” bins, where } 0^\circ < \alpha < 90^\circ)$$

$$f_{\text{perp},k} = 1/2\pi \sum_{m=10,19} [f_k(\alpha_m) \Omega_m], \text{ (“perpendicular” bins, where } 60^\circ < \alpha < 120^\circ)$$

$$f_{\text{anti},k} = 1/2\pi \sum_{m=15,29} [f_k(\alpha_m) \Omega_m], \text{ (“anti-parallel” bins, where } 90^\circ < \alpha < 180^\circ)$$

$$f_{\text{omni},k} = 1/4\pi \sum_{m=0,29} [f_k(\alpha_m) \Omega_m], \text{ (all bins, where } 0^\circ < \alpha < 180^\circ)$$

13 values of $f_{\text{para},k}$ ($f_{\text{para},0}, f_{\text{para},1}, \dots, f_{\text{para},12}$), along with the corresponding 13 values of $f_{\text{perp},k}$, $f_{\text{anti},k}$, and $f_{\text{omni},k}$ (available about every 12s) form this data product.

Data-product Files for this Mode

Each data-product described above is stored as both a “flat binary” file and a CDF file for each day of processed data. For reference, a typical day yields 6000-7000 energy “spectra” (about 1 every 12s, with data accumulated over 9s; accounting for “null spectra”, data gaps, etc.). Each non-null spectrum yields the set of values described above. Noting that the naming conventions are mostly historical in nature (with the exceptions of ‘h’ for “high resolution” and ‘m’ for “modified”, as in derived, in the CDF files), the files for each *yyyymmdd* date are named:

Product	Flat-binary filename	ISTP-compliant CDF filename
<i>Pitch-angle distributions</i>	<code>yyyymmdd_v06.pit</code>	<code>wi_h3_swe_yyyyymmdd_v01.cdf</code>
<i>Pitch-distrib. averages</i>	<code>yyyymmdd_v06.pitavg</code>	<code>wi_m0_swe_yyyyymmdd_v01.cdf</code>
<i>Strahl beam-descriptions</i>	<code>yyyymmdd_v08.str</code>	<code>wi_m1_swe_yyyyymmdd_v01.cdf</code>

Notes: The first date of processed new-mode data is *yyyymmdd*=**20020816**. While accessing the data from our flat-binary files requires the specialized software used internally by the SWE electron science team, the CDF files are self-describing and a variety of software tools exist for accessing their data.